Exact 3D Thermoelastic Solutions for a Penny-Shaped Crack in an Infinite Magnetoelectric Medium

Chen Weiqiu(陈伟球)*

Department of Engineering Mechanics, Zhejiang University, Hangzhou, 310027, P. R. China

(Received 20 October 2013; revised 26 November 2013; accepted 30 November 2013)

Abstract: Exact solutions of three-dimensional (3D) crack problems are much less in number than those of two-dimensional ones, especially for multi-field coupling media exhibiting a certain kind of material anisotropy. An exact 3D thermoelastic solution has been reported for a uniformly heated penny-shaped crack in an infinite magnetoelectric space, with impermeable electromagnetic conditions assumed on the crack faces. Exact 3D solutions for the penny-shaped crack subjected to uniform or point temperature load are further presented here when the crack faces are electrically and magnetically permeable. The solutions, obtained by the potential theory method, are exact in the sense that all field variables are explicitly derived and expressed in terms of elementary functions. Along with the previously reported solution, the limits or bounds of the stress intensity factor at the crack-tip for a practical crack can be identified.

Key words: magnetoelectric material; potential theory method; penny-shaped crack; general solution; exact three-dimensional solution

CLC number: O324 **Document code**: A **Article ID**: 1005-1120(2014)02-0119-09

1 Introduction

Magnetoelectric (ME) materials are a new type of functional materials, characterized by the unique magnetoelectric coupling (or simply the ME effect), which opens an avenue for many novel applications [1,2]. The single-phase ME materials usually possess a very low ME coefficient, and hence are impractical to be used in devices[3]. The composite ME materials consisting of both magnetic phase and electric phase exhibit a product ME effect, which is much stronger than the single-phase case[4]. The recent two decades have witnessed a fast growing research interest and outcome in the study of composite ME materials [5,6].

Composite ME materials are usually brittle in nature, and susceptible to damage caused by small cracks, voids and other defects. Thus, it is important to carry out a thorough study of crack problems in ME materials to obtain deep understanding of various coupling effects on their fracture behavior, wherein the mutual interactions among electric, magnetic and elastic fields should be considered. There already have been a lot of investigations on two-dimensional crack problems reported in Refs. [7-14], including in particular the first two pieces of work on thermal crack analysis by Gao et al[11,14]. The three-dimensional (3D) crack analysis also has attracted a certain amount of research attention. For instance, Zhao et al[15] discussed the permeability of electric and magnetic fields within the penny-shaped crack. Zhong and Li[16] further proposed a semi-permeable model for the electric and magnetic fields within the crack and studied its effect on the fracture behavior of a penny-shaped crack. A similar but independent research was reported by Wang et al[17]. The 3D dynamic fracture problem of a penny-shaped crack in an ME layer was considered by Feng et al[18]. There are only few works concerning 3D thermal crack analysis of ME materials, though as earlier in 2004, Chen et al[19]

* **Corresponding author**: Chen Weiqiu, Professor, E-mail: chenwq@zju. edu. cn.

derived an exact 3D solution for a penny-shaped crack embedded in an infinite ME medium subjected to a uniform temperature prescribed over the crack faces. Niraula and Wang[20] compared various field intensity factors for impermeable and permeable electric/magnetic conditions on the crack faces. A penny-shaped crack subjected to a uniform heat flux was later considered by Niraula and Wang[21]. In is noted that, unlike Ref. [19], Niraula and Wang[20,21] derived exact and explicit expressions only for the field intensity factors.

This paper is a supplement to our previous work[19], where impermeable electromagnetic conditions were assumed on the crack faces. For transversely isotropic ME materials, exact 3D expressions for all field variables are derived here for a penny-shaped crack subjected to uniform or point temperature load when both the electric and magnetic conditions on the crack faces become permeable. The solution strategy closely follows that in Ref. [19] by using the potential theory method and based on a concise general solution, which is expressed in terms of six quasi-harmonic functions. Such general solution was first suggested by Chen[22] for piezothermoelastic problem. It has been shown that the general solution is very useful, in conjunction with the potential theory method[23], in solving mixed boundary value problems for advanced materials with multi-field coupling. The present work is a further illustration of the versatility and elegancy of the general solution and the potential theory method.

2 Basic Equations and General Solution

The equations governing the thermo-mechanical behavior of a transversely isotropic ME medium with couplings among electric, magnetic, elastic and thermal fields can be written in Cartesian coordinates (x, y, z) in terms of mechanical displacements (u, v, w), electric potential (ϕ), magnetic potential (ψ) and temperature change (T) as follows

$$
\begin{aligned}
&\left(c_{11}\frac{\partial^2}{\partial x^2}+c_{66}\frac{\partial^2}{\partial y^2}+c_{44}\frac{\partial^2}{\partial z^2}\right)u+(c_{12}+c_{66})\frac{\partial^2 v}{\partial x\partial y}+\\
&\quad(c_{13}+c_{44})\frac{\partial^2 w}{\partial x\partial z}+(e_{15}+e_{31})\frac{\partial^2 \phi}{\partial x\partial z}+\\
&\quad(q_{15}+q_{31})\frac{\partial^2 \psi}{\partial x\partial z}-\beta_1\frac{\partial T}{\partial x}=0\\
&(c_{12}+c_{66})\frac{\partial^2 u}{\partial x\partial y}+\left(c_{66}\frac{\partial^2}{\partial x^2}+c_{11}\frac{\partial^2}{\partial y^2}+c_{44}\frac{\partial^2}{\partial z^2}\right)v+\\
&\quad(c_{13}+c_{44})\frac{\partial^2 w}{\partial y\partial z}+(e_{15}+e_{31})\frac{\partial^2 \phi}{\partial y\partial z}+\\
&\quad(q_{15}+q_{31})\frac{\partial^2 \psi}{\partial y\partial z}-\beta_1\frac{\partial T}{\partial y}=0\\
&(c_{13}+c_{44})\frac{\partial}{\partial z}\left(\frac{\partial u}{\partial x}+\frac{\partial v}{\partial y}\right)+\left(c_{44}\Delta+c_{33}\frac{\partial^2}{\partial z^2}\right)w+\\
&\quad\left(e_{15}\Delta+e_{33}\frac{\partial^2}{\partial z^2}\right)\phi+\left(q_{15}\Delta+q_{33}\frac{\partial^2}{\partial z^2}\right)\psi-\beta_3\frac{\partial T}{\partial z}=0\\
&(e_{15}+e_{31})\frac{\partial}{\partial z}\left(\frac{\partial u}{\partial x}+\frac{\partial v}{\partial y}\right)+\left(e_{15}\Delta+e_{33}\frac{\partial^2}{\partial z^2}\right)w-\\
&\quad\left(\varepsilon_{11}\Delta+\varepsilon_{33}\frac{\partial^2}{\partial z^2}\right)\phi-\left(d_{11}\Delta+d_{33}\frac{\partial^2}{\partial z^2}\right)\psi+\\
&\quad p_3\frac{\partial T}{\partial z}=0\\
&(q_{15}+q_{31})\frac{\partial}{\partial z}\left(\frac{\partial u}{\partial x}+\frac{\partial v}{\partial y}\right)+\left(q_{15}\Delta+q_{33}\frac{\partial^2}{\partial z^2}\right)w-\\
&\quad\left(d_{11}\Delta+d_{33}\frac{\partial^2}{\partial z^2}\right)\phi-\left(\mu_{11}\Delta+\mu_{33}\frac{\partial^2}{\partial z^2}\right)\psi+\\
&\quad\lambda_3\frac{\partial T}{\partial z}=0\\
&\left(k_{11}\Delta+k_{33}\frac{\partial^2}{\partial z^2}\right)T=0
\end{aligned}
\tag{1}
$$

where c_{ij}, ε_{ij}, e_{ij}, q_{ij}, d_{ij}, μ_{ij}, p_3 and λ_3 are the elastic, dielectric, piezoelectric, piezomagnetic, magnetoelectric, magnetic, pyroelectric and pyromagnetic constants, respectively; β_i and k_{ij} are the thermal moduli and coefficients of heat conduction, respectively. $\Delta=\partial^2/\partial x^2+\partial^2/\partial y^2$ is the two-dimensional Laplacian operator, and there is $c_{11}=c_{12}+2c_{66}$ for materials with transverse isotropy when the material axis of symmetry is perpendicular to the x-y plane.

By virtue of the operator theory, Chen et al[19] derived the following general solution to Eq. (1)

$$
\begin{aligned}
U&=-\Lambda\left(\sum_{i=1}^{5}\Psi_i+\mathrm{i}\Psi_0\right)\\
w_k&=\sum_{i=1}^{5}\alpha_{ik}\frac{\partial \Psi_i}{\partial z_i}\quad k=1,2,3\\
T&=\sum_{i=1}^{5}\alpha_{i4}\frac{\partial^2 \Psi_i}{\partial z_i^2}
\end{aligned}
\tag{2}
$$

where a complex and compact notation is employed with $U=u+\mathrm{i}v, w_1=w, w_2=\phi, w_3=\psi$, as well as $\Lambda=\partial/\partial x+\mathrm{i}\partial/\partial y$, here $\mathrm{i}=\sqrt{-1}$. α_{ij} are the combinations of material constants[19]. $z_i=s_i z$ with $s_0=\sqrt{c_{66}/c_{44}}$, $s_5=\sqrt{k_{11}/k_{33}}$, and $s_i\,(i=1,2,3,4)$ being the four roots (with positive real part) of the following algebraic equation

$$n_0 s^8-n_1 s^6+n_2 s^4-n_3 s^2+n_4=0 \qquad (3)$$

where n_i are also the combinations of material constants[19]. For simplicity, it is assumed that the four roots are distinct from each other, otherwise, the general solution should take the form different from Eq. (2).

The six functions Ψ_i ($i=0,1,\cdots,5$) in Eq. (2) are quasi-harmonic, satisfying

$$\left(\Delta+\frac{\partial^2}{\partial z_i^2}\right)\Psi_i=0 \qquad i=0,1,\cdots,5 \qquad (4)$$

With the general solution in Eq. (2), one can express stresses (σ_i, τ_{ij}), electric displacements (D_i), magnetic inductions (B_i), and heat fluxes (q_i) as

$$\sigma_{zk}=\sum_{i=1}^{5}\gamma_{ik}\frac{\partial^2\Psi_i}{\partial z_i^2} \qquad k=1,2,3,4$$

$$\sigma_2=-2c_{66}\Lambda^2\left(\sum_{i=1}^{5}\Psi_i+\mathrm{i}\Psi_0\right)$$

$$\tau_{zk}=\Lambda\left(\sum_{i=1}^{5}\gamma_{ik}s_i\frac{\partial\Psi_i}{\partial z_i}-\mathrm{i}s_0\nu_k\frac{\partial\Psi_0}{\partial z_0}\right) \qquad k=1,2,3 \quad (5)$$

$$q_h=k_{11}\sum_{i=1}^{5}\alpha_{i4}\Lambda\frac{\partial^2\Psi_i}{\partial z_i^2},\ q_z=k_{33}\sum_{i=1}^{5}\alpha_{i4}\frac{\partial^3\Psi_i}{\partial z_i^3}$$

where $\sigma_{z1}=\sigma_z$, $\sigma_{z2}=D_z$, $\sigma_{z3}=B_z$, $\sigma_{z4}=\sigma_x+\sigma_y$, $\sigma_2=\sigma_x-\sigma_y+2\mathrm{i}\tau_{xy}$, $\tau_{z1}=\tau_{xz}+\mathrm{i}\tau_{yz}$, $\tau_{z2}=D_x+\mathrm{i}D_y$, $\tau_{z3}=B_x+\mathrm{i}B_y$, $q_h=q_x+\mathrm{i}q_y$, and γ_{ik}, ν_k are the material coefficients defined in Ref. [19].

3 Boundary Value Problem and Potential Theory Method

Let us consider a flat crack S embedded in an infinite ME space, with its surface located in the x-y plane, see Fig. 1. An arbitrary temperature $\Theta(x,y)$ is assumed to be symmetrically prescribed over the upper and lower crack faces. In contrast to the impermeable electromagnetic conditions treated in Ref. [19], authors now assume that the normal components of electric displacement and magnetic induction, the electric potential, and the magnetic potential are all continuous across the crack, i. e.

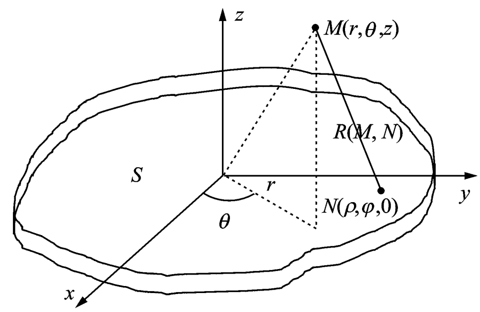

Fig. 1 Flat crack in infinite ME medium, occupying region S in x-y plane

$$\left.\begin{aligned}&D_z(x,y,0^+)=D_z(x,y,0^-)\\&\phi(x,y,0^+)=\phi(x,y,0^-)\\&B_z(x,y,0^+)=B_z(x,y,0^-)\\&\psi(x,y,0^+)=\psi(x,y,0^-)\end{aligned}\right\}\quad (x,y)\in S \qquad (6)$$

These are known as the permeable electromagnetic conditions on the crack faces[15].

By the symmetry consideration, the solution may be sought by solving the mixed boundary value problem of the half-space $z\geqslant 0$, with the following surface conditions at $z=0$

$$\begin{cases}\sigma_z=0,\ T=\Theta(x,y), & \text{for } (x,y)\in S\\ w=0,\ q_z=0, & \text{for } (x,y)\notin S\\ \phi=0,\ \psi=0, & \text{for } -\infty<(x,y)<\infty\\ \tau_{xz}=\tau_{yz}=0, & \text{for } -\infty<(x,y)<\infty\end{cases} \qquad (7)$$

Compared to the one for an impermeable crack[19], the most significant difference is that no jump of electric or magnetic potential takes place across the crack with permeable conditions, which leads to the assumption of the following quasi-harmonic functions

$$\Psi_0=0,\ \Psi_i(z)=h_{i1}H_1(z_i)+h_{i2}H_2(z_i) \qquad i=1,2,\cdots,5 \qquad (8)$$

where h_{ij} are constants to be determined, and

$$H_1(r,\theta,z)=\iint_S\frac{\omega(N)}{R(M,N)}\mathrm{d}S$$

$$H_2(r,\theta,z)=\iint_S\vartheta(N)\Big\{z\ln[R(M,N)+z]-R(M,N)\Big\}\mathrm{d}S \qquad (9)$$

where $\omega=w(x,y,0)$ and $\vartheta=\partial T(x,y,0)/\partial z$ are the displacement and temperature gradient on the crack surface, respectively. $R(M,N)$ is the distance between the points $M(r,\theta,z)$ and $N(\rho,\varphi,0)$, see Fig. 1. In the following, the cylindrical coordinates will be alternatively used for simplicity. In the above, the quasi-harmonic functions have been expressed in terms of two potentials, one itself being a standard potential of a single layer (PSL), and the other related to PSL by differentiation with respect to z twice.

To satisfy the fourth condition (i. e. the vanishing shear stress) in Eq. (7), it may take

$$\sum_{i=1}^{5}\gamma_{i1}s_i h_{ij}=0 \quad j=1,2 \tag{10}$$

It is known from the property of the potential of a simple layer[19,23] that

$$\begin{cases}(x,y)\notin S:\ \dfrac{\partial H_1}{\partial z}\bigg|_{z=0}=0,\ \dfrac{\partial^3 H_2}{\partial z^3}\bigg|_{z=0}=0\\ (x,y)\in S:\ \dfrac{\partial H_1}{\partial z}\bigg|_{z=0}=-2\pi\omega,\ \dfrac{\partial^3 H_2}{\partial z^3}\bigg|_{z=0}=-2\pi\vartheta\end{cases} \tag{11}$$

Thus, the second and third conditions in Eq. (7) give rise to the equations

$$\sum_{i=1}^{5}\alpha_{i1}h_{ij}=-\frac{\delta_{1j}}{2\pi},\ \sum_{i=1}^{5}\alpha_{i2}h_{ij}=0$$
$$\sum_{i=1}^{5}\alpha_{i3}h_{ij}=0,\ \sum_{i=1}^{5}\alpha_{i4}s_i h_{ij}=-\frac{\delta_{2j}}{2\pi} \quad j=1,2 \tag{12}$$

Now the constants h_{ij} can be determined from Eqs. (10,12) as

$$\begin{Bmatrix}h_{1j}\\h_{2j}\\h_{3j}\\h_{4j}\\h_{5j}\end{Bmatrix}=-\frac{1}{2\pi}\cdot$$
$$\begin{bmatrix}\gamma_{11}s_1 & \gamma_{21}s_2 & \gamma_{31}s_3 & \gamma_{41}s_4 & \gamma_{51}s_5\\ \alpha_{11} & \alpha_{21} & \alpha_{31} & \alpha_{41} & \alpha_{51}\\ \alpha_{12} & \alpha_{22} & \alpha_{32} & \alpha_{42} & \alpha_{52}\\ \alpha_{13} & \alpha_{23} & \alpha_{33} & \alpha_{43} & \alpha_{53}\\ \alpha_{14}s_1 & \alpha_{24}s_2 & \alpha_{34}s_3 & \alpha_{44}s_4 & \alpha_{54}s_5\end{bmatrix}^{-1}\begin{Bmatrix}0\\ \delta_{1j}\\ 0\\ 0\\ \delta_{2j}\end{Bmatrix}$$
$$j=1,2 \tag{13}$$

Finally, in view of the first condition in Eq. (13), we can get

$$g_{11}\Delta\iint_S\frac{\omega(N)}{R(N_0,N)}\mathrm{d}S-g_{12}\iint_S\frac{\vartheta(N)}{R(N_0,N)}\mathrm{d}S=0 \tag{14}$$

$$\iint_S\frac{\vartheta(N)}{R(N_0,N)}\mathrm{d}S=-2\pi s_5\Theta(N_0) \tag{15}$$

where $g_{1j}=\sum_{i=1}^{5}\gamma_{i1}h_{ij}\,(j=1,2)$, and $R(N_0,N)$ indicates the distance between two points N_0 and N, N_0, $N\in S$. In view of Eq. (15), Eq. (14) can be further rewritten as

$$\Delta\iint_S\frac{\omega(N)}{R(N_0,N)}\mathrm{d}S=-2\pi s_5 g_{12}\Theta(N_0)/g_{11} \tag{16}$$

It is seen that the integro-differential equation (16) and the integral equation (15) derived above for the permeable electromagnetic conditions have the same structures as those for the impermeable electromagnetic conditions presented in Ref. [19]. The difference between the two is clear, that is, for the permeable electromagnetic conditions there is only one integro-differential equation, while for the impermeable electromagnetic conditions, there are three such equations. However, the difficulty in solving these equations is at the same level because of the identical mathematical structure.

4 Exact Solutions for a Penny-Shaped Crack

When the crack occupies a circular region of radius a, we have a penny-shaped crack. In this case, Eqs. (15,16) can be written as

$$\int_0^{2\pi}\int_0^a\frac{\vartheta(\rho,\varphi)}{R_h}\rho\,\mathrm{d}\rho\mathrm{d}\varphi=-2\pi s_5\Theta(\rho_0,\varphi_0) \tag{17}$$

$$\Delta\iint_S\frac{\omega(\rho,\varphi)}{R_h}\rho\,\mathrm{d}\rho\mathrm{d}\varphi=-2\pi s_5 g_{12}\Theta(\rho_0,\varphi_0)/g_{11} \tag{18}$$

where $R_h=R(N_0,N)=\sqrt{\rho^2+\rho_0^2-2\cos(\varphi-\varphi_0)}$.

The solutions to Eqs. (17, 18) can be obtained by directly invoking Fabrikant′s results [23]

$$\omega(\rho,\varphi)=\frac{s_5 g_{12}}{\pi^2 g_{11}}\int_0^{2\pi}\int_0^a\frac{1}{R_h}\arctan\left(\frac{\eta}{R_h}\right)\Theta(\rho_0,\varphi_0)\rho_0\,\mathrm{d}\rho_0\mathrm{d}\varphi_0 \tag{19}$$

$$\vartheta(\rho,\varphi)=\frac{2s_5}{\pi\rho}L(\rho)\frac{\mathrm{d}}{\mathrm{d}\rho}\int_\rho^a\frac{x\,\mathrm{d}x}{(x^2-\rho^2)^{1/2}}\cdot L\left(\frac{1}{x^2}\right)\frac{\mathrm{d}}{\mathrm{d}x}\int_0^x\frac{\rho_0\,\mathrm{d}\rho_0}{(x^2-\rho_0^2)^{1/2}}L(\rho_0)\Theta(\rho_0,\varphi) \tag{20}$$

where $\eta=\sqrt{a^2-\rho^2}\sqrt{a^2-\rho_0^2}/a$, and $L(\cdot)$ is an operator defined as

$$L(k)f(\varphi)=\frac{1}{2\pi}\int_0^{2\pi}\frac{(1-k^2)f(\varphi_0)}{1+k^2-2k\cos(\varphi-\varphi_0)}\mathrm{d}\varphi_0 \tag{21}$$

In the case of thermoelasticity without coupling to the electric and magnetic fields, Chen et al[24] showed that exact solutions could be obtained when the temperature is prescribed on a single point or uniformly over the whole crack surface. In Ref. [19], only the solution for the uniform temperature was given. In the following, however, both solutions will be presented for the permeable electromagnetic conditions.

4.1 Uniform temperature

If the temperature prescribed on the crack surface is uniform, we have $\Theta(\rho,\varphi)=T_0$, where T_0 is a constant. Then, it can be obtained from Eqs. (19,20)

$$\vartheta(\rho,\varphi)=-\frac{2s_5T_0}{\pi\sqrt{a^2-r^2}}$$

$$\omega(\rho,\varphi)=\frac{2s_5g_{12}T_0}{\pi g_{11}}\sqrt{a^2-\rho^2} \tag{22}$$

Substituting the above results in Eq. (9) gives

$$H_1(r,\theta,z)=\frac{s_5g_{12}T_0}{g_{11}}\left[(2a^2+2z^2-r^2)\cdot\arcsin\left(\frac{a}{l_2}\right)-\frac{2a^2-3l_1^2}{a}\sqrt{l_2^2-a^2}\right]$$

$$H_2(r,\theta,z)=-2s_5T_0\left[\left(z^2-a^2-\frac{r^2}{2}\right)\cdot\arcsin\left(\frac{a}{l_2}\right)-\frac{3(2a^2-l_1^2)}{2a}\sqrt{l_2^2-a^2}+2az\ln(l_2+\sqrt{l_2^2-r^2})\right] \tag{23}$$

where

$$l_1=\frac{1}{2}[\sqrt{(r+a)^2+z^2}-\sqrt{(r-a)^2+z^2}]$$

$$l_2=\frac{1}{2}[\sqrt{(r+a)^2+z^2}+\sqrt{(r-a)^2+z^2}] \tag{24}$$

Here l_1, l_2 are the two length parameters that play important roles in expressing the analytical solutions in terms of elementary functions[23].

With H_1 and H_2 given in Eq. (23), the elastic, electric, magnetic and thermal fields can be obtained simply by differentiation

$$U=-\frac{2s_5g_{12}T_0}{g_{11}}re^{i\theta}\sum_{i=1}^{5}h_{i1}\left[\frac{a\sqrt{l_{2i}^2-a^2}}{l_{2i}^2}-\arcsin\left(\frac{a}{l_{2i}}\right)\right]-4s_5T_0\frac{e^{i\theta}}{r}\sum_{i=1}^{5}h_{i2}\cdot\left[\sqrt{l_{2i}^2-a^2}\left(a-\frac{l_{1i}^2}{2a}\right)-z_ia+\frac{r^2}{2}\arcsin\left(\frac{a}{l_{2i}}\right)\right]$$

$$w_k=\frac{4s_5g_{12}T_0}{g_{11}}\sum_{i=1}^{5}\alpha_{ik}h_{i1}\left[z_i\arcsin\left(\frac{a}{l_{2i}}\right)-\sqrt{a^2-l_{1i}^2}\right]-4s_5T_0\sum_{i=1}^{5}\alpha_{ik}h_{i2}\left[z_i\arcsin\left(\frac{a}{l_{2i}}\right)-\sqrt{a^2-l_{1i}^2}+a\ln(l_{2i}+\sqrt{l_{2i}^2-r^2})\right]\quad k=1,2,3$$

$$\sigma_{zk}=\frac{4s_5g_{12}T_0}{g_{11}}\sum_{i=1}^{5}\gamma_{ik}h_{i1}\left[\arcsin\left(\frac{a}{l_{2i}}\right)-\frac{a\sqrt{l_{2i}^2-a^2}}{l_{2i}^2-l_{1i}^2}\right]-4s_5T_0\sum_{i=1}^{5}\gamma_{ik}h_{i2}\arcsin\left(\frac{a}{l_{2i}}\right)\quad k=1,2,3,4$$

$$\sigma_2=-\frac{8c_{66}s_5g_{12}T_0}{g_{11}}ae^{i2\theta}\sum_{i=1}^{5}h_{i1}\frac{l_{1i}^2\sqrt{l_{2i}^2-a^2}}{l_{2i}^2(l_{2i}^2-l_{1i}^2)}+4c_{66}s_5T_0\frac{e^{i2\theta}}{r^2}\sum_{i=1}^{5}h_{i2}\left(a\sqrt{l_{2i}^2-a^2}+z_i\sqrt{a^2-l_{1i}^2}-2z_ia\right) \tag{25}$$

$$\tau_{zk}=\frac{4s_5g_{12}T_0}{g_{11}}a^2re^{i\theta}\sum_{i=1}^{5}\gamma_{ik}s_ih_{i1}\frac{\sqrt{a^2-l_{1i}^2}}{l_{2i}^2(l_{2i}^2-l_{1i}^2)}+4s_5T_0\frac{e^{i\theta}}{r}\sum_{i=1}^{5}\gamma_{ik}s_ih_{i2}(\sqrt{a^2-l_{1i}^2}-a)\quad k=1,2,3$$

$$T=\frac{4s_5g_{12}T_0}{g_{11}}\sum_{i=1}^{5}\alpha_{i4}h_{i1}\left[\arcsin\left(\frac{a}{l_{2i}}\right)-\frac{a\sqrt{l_{2i}^2-a^2}}{l_{2i}^2-l_{1i}^2}\right]-4s_5T_0\sum_{i=1}^{5}\alpha_{i4}h_{i2}\arcsin\left(\frac{a}{l_{2i}}\right)$$

$$q_h=\frac{4s_5k_{11}g_{12}T_0}{g_{11}}a^2re^{i\theta}\sum_{i=1}^{5}\alpha_{i4}h_{i1}\cdot\frac{z_i}{(l_{2i}^2-l_{1i}^2)^2\sqrt{a^2-l_{1i}^2}}\left[\frac{l_{1i}^2}{l_{2i}^2}-\frac{4(a^2-l_{1i}^2)}{(l_{2i}^2-l_{1i}^2)}\right]+4s_5k_{11}T_0\frac{e^{i\theta}}{r}\sum_{i=1}^{5}\alpha_{i4}h_{i2}\frac{z_il_{1i}^2}{(l_{2i}^2-l_{1i}^2)\sqrt{a^2-l_{1i}^2}}$$

$$q_z=\frac{4s_5k_{33}g_{12}T_0}{g_{11}}\sum_{i=1}^{5}\alpha_{i4}h_{i1}\frac{az_i}{(l_{2i}^2-l_{1i}^2)^2\sqrt{l_{2i}^2-a^2}}\cdot\left[\frac{4(l_{2i}^2-a^2)l_{1i}^2}{l_{2i}^2-l_{1i}^2}+l_{1i}^2-2a^2\right]+4s_5k_{33}T_0\cdot\sum_{i=1}^{5}\alpha_{i4}h_{i2}\frac{az_i}{(l_{2i}^2-l_{1i}^2)\sqrt{l_{2i}^2-a^2}}$$

where $l_{1i}=\frac{1}{2}[\sqrt{(r+a)^2+z_i^2}-\sqrt{(r-a)^2+z_i^2}]$,

$l_{2i}=\frac{1}{2}[\sqrt{(r+a)^2+z_i^2}+\sqrt{(r-a)^2+z_i^2}]$.

4.2 Point temperature

For the case when temperature vanishes everywhere except the point $(r_0,\theta_0,0)$, the exact solution can also be derived by making use of the results obtained in Ref. [24]. To proceed, let us divide the solution into two parts: one corresponds to H_1, and the other to H_2. The first part, discriminated by the superscript "(1)", is then given by

$$
\begin{aligned}
&U^{(1)}=-\frac{2s_5 g_{12}}{\pi g_{11}}\sum_{i=1}^{5}h_{i1}f_1(z_i)\Theta_0\\
&w_k^{(1)}=-\frac{2s_5 g_{12}}{\pi g_{11}}\sum_{i=1}^{5}\alpha_{i1}h_{i1}f_2(z_i)\Theta_0\quad k=1,2,3\\
&\sigma_{zk}^{(1)}=\frac{2s_5 g_{12}}{\pi g_{11}}\sum_{i=1}^{5}\gamma_{ik}h_{i1}f_3(z_i)\Theta_0\quad k=1,2,3,4\\
&\sigma_2^{(1)}=-\frac{4s_5 g_{12}c_{66}}{\pi g_{11}}\sum_{i=1}^{5}h_{i1}f_4(z_i)\Theta_0\\
&\tau_{zk}^{(1)}=\frac{2s_5 g_{12}}{\pi g_{11}}\sum_{i=1}^{5}\gamma_{ik}s_i h_{i1}f_5(z_i)\Theta_0\\
&T^{(1)}=\frac{2s_5 g_{12}}{g_{11}\pi}\sum_{i=1}^{5}\alpha_{i4}h_{i1}f_3(z_i)\Theta_0\\
&q_h^{(1)}=\frac{2s_5 k_{11}g_{12}}{\pi g_{11}}\sum_{i=1}^{5}\alpha_{i4}h_{i1}f_6(z_i)\Theta_0\\
&q_z^{(1)}=\frac{2s_5 k_{33}g_{12}}{g_{11}\pi}\sum_{i=1}^{5}\alpha_{i4}h_{i1}f_7(z_i)\Theta_0
\end{aligned}\tag{26}
$$

where Θ_0 is the magnitude of temperature at the application point $(r_0,\theta_0,0)$, and $f_i(z)$ are given by

$$
\begin{aligned}
&f_1(z)=\frac{1}{\bar t}\left[\frac{z}{R_0}\arctan\left(\frac{h}{R_0}\right)-\frac{\sqrt{a^2-r_0^2}}{\bar s}\cdot\arctan\left(\frac{\bar s}{\sqrt{l_2^2-a^2}}\right)\right]\\
&f_2(z)=\frac{1}{R_0}\arctan\left(\frac{h}{R_0}\right)\\
&f_3(z)=\frac{z}{R_0^3}\arctan\left(\frac{h}{R_0}\right)-\frac{h}{z(R_0^2+h^2)}\left(\frac{r^2-l_1^2}{l_2^2-l_1^2}-\frac{z^2}{R_0^2}\right)\\
&f_4(z)=\frac{\sqrt{a^2-r_0^2}}{\bar t\bar s}\left(\frac{2}{\bar t}-\frac{r_0 e^{i\theta_0}}{\bar s^2}\right)\arctan\left(\frac{\bar s}{\sqrt{l_2^2-a^2}}\right)-\frac{z(3R_0^2-z^2)}{\bar t^2R_0^3}\arctan\left(\frac{h}{R_0}\right)+\\
&\qquad\frac{\sqrt{a^2-r_0^2}\sqrt{l_2^2-a^2}\,r_0 e^{i\theta_0}}{\bar t\bar s^2[l_2^2-rr_0e^{-i(\theta-\theta_0)}]}-\frac{zh}{R_0^2+h^2}\left[\frac{t}{\bar tR_0^2}-\frac{r^2e^{i2\theta}}{(l_2^2-l_1^2)(l_2^2-r^2)}\right]\\
&f_5(z)=\frac{t}{R_0^3}\arctan\left(\frac{h}{R_0}\right)+\frac{h}{R_0^2+h^2}\left(\frac{re^{i\theta}}{l_2^2-l_1^2}+\frac{t}{R_0^2}\right)\\
&f_6(z)=-\frac{3tz}{R_0^5}\arctan\left(\frac{h}{R_0}\right)+\frac{thz}{R_0^2(R_0^2+h^2)}\cdot\left[\frac{l_1^2}{(l_2^2-l_1^2)(a^2-l_1^2)}-\frac{1}{R_0^2}\right]+\\
&\qquad\frac{l_1^2hz}{(R_0^2+h^2)(l_2^2-l_1^2)(a^2-l_1^2)}\left(\frac{re^{i\theta}}{l_2^2-l_1^2}+\frac{t}{R_0^2}\right)-\frac{2hz}{(R_0^2+h^2)^2}\left(1+\frac{h^2l_1^2}{(l_2^2-l_1^2)(a^2-l_1^2)}\right)\left(\frac{re^{i\theta}}{l_2^2-l_1^2}+\frac{t}{R_0^2}\right)-\\
&\qquad\frac{2hz}{R_0^2+h^2}\left[\frac{re^{i\theta}}{(l_2^2-l_1^2)^3}(l_2^2+l_1^2)+\frac{t}{R_0^4}\right]\\
&f_7(z)=\frac{R_0^2-3z^2}{R_0^5}\arctan\left(\frac{h}{R_0}\right)+\frac{hz^2}{R_0^2(R_0^2+h^2)}\left[\frac{l_1^2}{(l_2^2-l_1^2)(a^2-l_1^2)}-\frac{1}{R_0^2}\right]-\\
&\qquad\frac{l_1^2h}{(R_0^2+h^2)(l_2^2-l_1^2)(a^2-l_1^2)}\cdot\left(\frac{r^2-l_1^2}{l_2^2-l_1^2}-\frac{z^2}{R_0^2}\right)+\frac{h}{z^2(R_0^2+h^2)}\left(\frac{r^2-l_1^2}{l_2^2-l_1^2}-\frac{z^2}{R_0^2}\right)+\\
&\qquad\frac{2h}{(R_0^2+h^2)^2}\left[1+\frac{l_1^2h^2}{(l_2^2-l_1^2)(a^2-l_1^2)}\right]\cdot\left(\frac{r^2-l_1^2}{l_2^2-l_1^2}-\frac{z^2}{R_0^2}\right)-\frac{2h}{(R_0^2+h^2)}\cdot\\
&\qquad\left[\frac{l_1^2}{(l_2^2-l_1^2)^2}-\frac{r^2-l_1^2}{(l_2^2-l_1^2)^3}(l_2^2+l_1^2)-\frac{R_0^2-z^2}{R_0^4}\right]
\end{aligned}\tag{27}
$$

with

$$t=re^{i\theta}-r_0e^{i\theta_0},\ \bar s=\sqrt{a^2-rr_0e^{-i(\theta-\theta_0)}}$$

$$h=\sqrt{a^2-l_1^2}\sqrt{a^2-r_0^2}/a$$

$$R_0=\sqrt{r^2+r_0^2-2rr_0\cos(\theta-\theta_0)+z^2}$$

The second part, discriminated by the superscript "(2)", is given as

$$
\begin{aligned}
&U^{(2)}=\frac{2s_5}{\pi}\sum_{i=1}^{5}h_{i2}g_1(z_i)\Theta_0\\
&w_k^{(2)}=-\frac{2s_5}{\pi}\sum_{i=1}^{5}\alpha_{ik}h_{i2}g_2(z_i)\Theta_0\quad k=1,2,3\\
&\sigma_{zk}^{(2)}=-\frac{2s_5}{\pi}\sum_{i=1}^{5}\gamma_{ik}h_{i2}g_3(z_i)\Theta_0\quad k=1,2,3,4\\
&\sigma_2^{(2)}=\frac{4s_5c_{66}}{\pi}\sum_{i=1}^{5}h_{i2}g_4(z_i)\Theta_0\\
&\tau_{zk}^{(2)}=-\frac{2s_5}{\pi}\sum_{i=1}^{5}\gamma_{ik}s_ih_{i2}g_5(z_i)\Theta_0\quad k=1,2,3\\
&T^{(2)}=-\frac{2s_5}{\pi}\sum_{i=1}^{5}\alpha_{i4}h_{i2}g_3(z_i)\Theta_0\\
&q_h^{(2)}=-\frac{2k_{11}s_5}{\pi}\sum_{i=1}^{5}\alpha_{i4}h_{i2}g_6(z_i)\Theta_0\\
&q_z^{(2)}=-\frac{2k_{33}s_5}{\pi}\sum_{i=1}^{5}\alpha_{i4}h_{i2}g_7(z_i)\Theta_0
\end{aligned}\tag{28}
$$

where

$$g_1(z)=\frac{1}{\bar t}\left\{\frac{z}{R_0}\arctan\left(\frac{h}{R_0}\right)-\frac{z}{h}+\frac{1}{\sqrt{a^2-r_0^2}}\cdot\left[\sqrt{a^2-r^2/\zeta}\arctan\left(\frac{a\sqrt{r^2-l_1^2}}{l_1\sqrt{a^2-r^2/\zeta}}\right)+\right.\right.$$

$$\frac{\pi}{2}\sqrt{a^2-r^2/\bar{\zeta}}-\frac{z}{\sqrt{\bar{\zeta}-1}}\arctan\left(\frac{\sqrt{a^2-l_1^2}}{a\sqrt{\bar{\zeta}-1}}\right)\Bigg]\Bigg]\Bigg\},$$

$$g_2(z)=-\frac{1}{R_0}\arctan\left(\frac{h}{R_0}\right)+\frac{1}{\sqrt{a^2-r_0^2}}\cdot$$

$$\left[\ln\left(\frac{a+\sqrt{a^2-l_1^2}}{l_1}\right)+\frac{1}{\sqrt{\zeta-1}}\arctan\left(\frac{\sqrt{a^2-l_1^2}}{a\sqrt{\zeta-1}}\right)+\right.$$

$$\left.\frac{1}{\sqrt{\bar{\zeta}-1}}\arctan\left(\frac{\sqrt{a^2-l_1^2}}{a\sqrt{\bar{\zeta}-1}}\right)\right]$$

$$g_3(z)=\frac{z}{R_0^3}\left[\frac{R_0}{h}+\arctan\left(\frac{h}{R_0}\right)\right]$$

$$g_4(z)=-\frac{z(3R_0^2-z^2)}{\bar{t}^2R_0^3}\arctan\left(\frac{h}{R_0}\right)+\frac{z}{\bar{t}}\cdot$$

$$\left[\frac{2}{\bar{t}h}-\frac{ht}{R_0^2(R_0^2+h^2)}\right]-\frac{ze^{i\varphi}(r^2-r_0^2\zeta)}{\bar{t}hr(R_0^2+h^2)}-$$

$$\frac{1}{\bar{t}^2}\left(\frac{\sqrt{a^2-r_0^2}}{\sqrt{a^2-r^2/\zeta}}+\frac{\sqrt{a^2-r^2/\zeta}}{\sqrt{a^2-r_0^2}}\right)\cdot$$

$$\arctan\left(\frac{a\sqrt{r^2-l_1^2}}{l_1\sqrt{a^2-r^2/\zeta}}\right)+\frac{3z}{\bar{t}^2\sqrt{a^2-r_0^2}\sqrt{\bar{\zeta}-1}}\cdot$$

$$\arctan\left(\frac{\sqrt{a^2-l_1^2}}{a\sqrt{\bar{\zeta}-1}}\right)+\frac{z}{\bar{t}^2h}\left[\frac{l_1^2(1-1/\bar{\zeta})}{a^2\zeta-l_1^2}+\frac{a^2-l_1^2}{a^2\bar{\zeta}-l_1^2}\right]-$$

$$\frac{\pi}{\bar{t}^2\sqrt{a^2-r_0^2}}\sqrt{a^2-r^2/\bar{\zeta}} \tag{29}$$

$$g_5(z)=\frac{t}{R_0^3}\arctan\left(\frac{h}{R_0}\right)-\frac{z^2}{h\bar{t}R_0^2}-\frac{1}{\sqrt{a^2-r_0^2}\,\bar{t}\sqrt{\bar{\zeta}-1}}\cdot$$

$$\arctan\left(\frac{\sqrt{a^2-l_1^2}}{a\sqrt{\bar{\zeta}-1}}\right)$$

$$g_6(z)=-\frac{3tz}{R_0^5}\arctan\left(\frac{h}{R_0}\right)+\frac{thz}{R_0^2(R_0^2+h^2)}\cdot$$

$$\left[\frac{l_1^2}{(l_2^2-l_1^2)(a^2-l_1^2)}-\frac{1}{R_0^2}\right]-\frac{2z}{h\bar{t}R_0^4}(R_0^2-z^2)+$$

$$\frac{z^3l_1^2}{h\bar{t}R_0^2(l_2^2-l_1^2)(a^2-l_1^2)}-\frac{zl_1^2}{h\bar{t}(a^2\bar{\zeta}-l_1^2)(l_2^2-l_1^2)}$$

$$g_7(z)=\frac{R_0^2-3z^2}{R_0^5}\left[\frac{R_0}{h}+\arctan\left(\frac{h}{R_0}\right)\right]-$$

$$\frac{z^2}{h(R_0^2+h^2)}\left[\frac{l_1^2}{(l_2^2-l_1^2)(a^2-l_1^2)}-\frac{1}{R_0^2}\right]$$

where $\zeta = re^{i(\theta-\theta_0)}/r_0$. The summation of Eqs. (26, 28) gives the complete solution for the point temperature load case.

5 Stress Intensity Factor

It's important and also interesting to study the singular behavior of the stress field at the crack tip. Noticing the following properties

$$z=0:\ l_1\rightarrow\min(a,r),\ \text{and}\ l_2\rightarrow\max(a,r) \tag{30}$$

one gains, for the uniform temperature, from Eq. (25)

$$\sigma_z\big|_{z=0}=\begin{cases}-4s_5g_{12}T_0a\dfrac{1}{\sqrt{r^2-a^2}} & r\geqslant a\\ 0 & r>a\end{cases} \tag{31}$$

and, for the point temperature, from Eqs. (26, 28)

$$\sigma_z\big|_{z=0}=\begin{cases}-\dfrac{2s_5g_{12}}{\pi}\dfrac{1}{\sqrt{r^2-a^2}}\cdot\\ \qquad\dfrac{\sqrt{a^2-r_0^2}}{r^2+r_0^2-2rr_0\cos(\theta-\theta_0)}\Theta_0 & r\geqslant a\\ 0 & r<a\end{cases} \tag{32}$$

In the above derivation, the following property has been utilized

$$\begin{aligned}&\lim_{z\to0}f_3(z)=-\sqrt{\frac{a^2-r_0^2}{r^2-a^2}}\frac{1}{r^2+r_0^2-2rr_0\cos(\theta-\theta_0)}\\&\lim_{z\to0}g_3(z)=\sqrt{\frac{r^2-a^2}{a^2-r_0^2}}\frac{1}{r^2+r_0^2-2rr_0\cos(\theta-\theta_0)}\end{aligned} \tag{33}$$

It can be seen that the normal stress σ_z vanishes at the crack surface for $r<a$, which is just required by one of the conditions in Eq. (7). This agreement could be a partial verification of the current theoretical analysis. Moreover, the expression of σ_z for $r\geqslant a$ is found to be identical to that obtained by Tsai[25] in the thermoelastic case, thereby giving another strong support of our results. It is also noted that the expression in Eq. (31) can be obtained by simply integrating Eq. (32) over the crack face.

If the stress intensity factor is defined as

$$K_I=\lim_{r\to a}\left\{\sqrt{2\pi(r-a)}\,\sigma_z\big|_{z=0}\right\} \tag{34}$$

then for the uniform temperature one gets

$$K_I=-4s_5\sqrt{\pi a_0}\,g_{12}T_0 \tag{35}$$

and for the point temperature

$$K_I=-\frac{2s_5g_{12}}{\sqrt{\pi a}}\Theta_0\frac{\sqrt{a^2-r_0^2}}{a^2+r_0^2-2ar_0\cos(\theta-\theta_0)} \tag{36}$$

Note that Eq. (35) can be obtained from Eq. (36) by simple integration.

The stress intensity factors derived above are identical to those in form for the thermoelastic case[24]. However, due to the multi-field coupling in an ME material, the value of the material constant g_{12} appearing in the stress intensity factor will be different from that in the elastic counterpart of the ME material.

6 Conclusions

This paper addresses the problem of an electrically and magnetically permeable penny-shaped crack in an infinite transversely isotropic magnetoelectric medium. By employing the potential theory method, the exact 3D solutions are derived when uniform or point temperature is prescribed on the crack faces. Both solutions are expressed in terms of elementary functions.

The results obtained in this paper should serve as a necessary supplement to our previous work[19], which assumes impermeable electromagnetic conditions on the crack surface. Further comparison shows that:

(1) For the impermeable electromagnetic conditions, the electric and magnetic fields also experience singularities at the crack tip, while for the permeable electromagnetic conditions these fields are no longer singular at the crack tip because of the continuity conditions specified in Eq. (6);

(2) The stress intensity factors for the two different and idealized electromagnetic conditions provide the upper and lower limits of an actual situation.

The present analysis can be further extended to the case in which either the electric or magnetic field (but not simultaneously) is permeable on the crack faces. It is also interesting to consider a problem of cracks subjected to heat flux rather than temperature as discussed in this paper.

Acknowledgements

This work was supported by the National Natural Science Foundation of China (11321202) and the Specialized Research Fund for the Doctoral Program of Higher Education (2013010 1110120).

References:

[1] Spaldin N A, Fiebig M. The renaissance of magnetoelectric multiferroics[J]. Science, 2005, 309: 391-392.

[2] Eerenstein W, Mathur N D, Scott J F. Multiferroic and magnetoelectric materials[J]. Nature, 2006, 442: 759-765.

[3] Rado G T, Folen V J. Observation of the magnetically induced magnetoelectric effect and evidence for antiferromagnetic domains[J]. Physics Review Letters, 1961,7: 310-311.

[4] Van Suchtelen J. Product properties: A new application of composite materials[J]. Philips Research Reports, 1972, 27: 28-37

[5] Nan C W, Bichurin M I, Dong S X, et al. Multiferroic magnetoelectric composites historical perspective, status, multiferroic magnetoelectric composites: Historical perspective, status, and future directions[J]. Journal of Applied Physics, 2008, 103: 031101.

[6] Zhai J Y, Xing Z P, Dong S X, et al. Magnetoelectric laminate composites: An overview[J]. Journal of American Ceramic Society, 2008,91: 351-358.

[7] Li X F. Dynamic analysis of a cracked magnetoelectroelastic medium under antiplane mechanical and inplane electric magnetic impacts [J]. International Journal of Solids and Structures, 2001, 42: 3185-3205.

[8] Liu J X, Liu X L, Zhao Y B. Green′s functions for anisotropic magnetoelectroelastic solids with an elliptical cavity or a crack[J]. International Journal of Engineering Science, 2001,39: 1405-1418.

[9] Gao C F, Kessler H, Balke H. Crack problems in magnetoelectroelastic solids. Part I: Exact solution of a crack[J]. International Journal of Engineering Science, 2003,41:969-981.

[10] Gao C F, Kessler H, Balke H. Crack problems in magnetoelectroelastic solids. Part II: General solution of collinear cracks[J]. International Journal of Engineering Science, 2003,41: 983-994.

[11] Gao C F, Kessler H, Balke H. Fracture analysis of electromagnetic thermoelastic solids [J]. European Journal of Mechanics, A/Solids, 2003,22: 433-442.

[12] Gao C F, Tong P, Zhang T Y. Interfacial crack problems in magneto-electric solids[J]. International Journal of Engineering Science, 2003,41: 2105-2121.

[13] Gao C F, Tong P, Zhang T Y. Fracture mechanics for a mode III crack in a magnetoelectroelastic solid [J]. International Journal of Solids and Structures, 2004,41: 6613-6629.

[14] Gao C F, Noda N. Thermal-induced interfacial cracking of magnetoelectroelastic material[J]. International Journal of Engineering Science, 2004, 42: 1347-1360.

[15] Zhao M H, Yang F, Liu T. Analysis of a penny-shaped crack in a magneto-electro-elastic medium[J]. Philosophical Magazine, 2006,86: 4397-4416.

[16] Zhong X C, Li X F. Fracture analysis of a magneto-

electroelastic solid with a penny-shaped crack by considering the effects of the opening crack interior[J]. International Journal of Engineering Science, 2008, 46: 374-390.

[17] Wang B L, Sun Y G, Zhang H Y. Analysis of a penny-shaped crack in magnetoelectroelastic materials [J]. Journal of Applied Physics, 2008, 103: 083530.

[18] Feng W J, Pan E, Wang X. Dynamic fracture analysis of a penny-shaped crack in a magnetoelectroelastic layer[J]. International Journal of Solids and Structures, 2007, 44: 7955-7974.

[19] Chen W Q, Lee K Y, Ding H J. General solution for transversely isotropic magneto-electro-thermo-elasticity and the potential theory method[J]. International Journal of Engineering Science, 2004, 42: 1361-1379.

[20] Niraula O P, Wang B L. A magneto-electro-elastic material with a penny-shaped crack subjected to temperature loading[J]. Acta Mechanica, 2006, 187: 151-168.

[21] Niraula O P, Wang B L. Thermal stress analysis in magneto-electro-thermo-elasticity with a penny-shaped crack under uniform heat flow[J]. Journal of Thermal Stresses, 2006, 29: 423-437.

[22] Chen W Q. On the general solution for piezothermoelasticity for transverse isotropy with application [J]. Journal of Applied Mechanics, 2000, 67(4): 705-711.

[23] Fabrikant V I. Applications of potential theory in mechanics[M]. Dordrecht, Netherlands: Kluwer, 1989.

[24] Chen W Q, Ding H J, Ling D S. Thermoelastic field of a transversely isotropic elastic medium containing a penny-shaped crack: Exact fundamental solution[J]. International Journal of Solids and Structures, 2004, 41(1): 69-83.

[25] Tsai Y M. Thermal stress in a transversely isotropic medium containing a penny-shaped crack[J]. Journal of Applied Mechanics, 1983, 50(1): 24-28.

(Executive editor: Zhang Tong)